

Crystal Structure of *Escherichia coli* GroEL in Substrate and ADP Unloaded State

Sitaram Meena and Ajay K Saxena*

Structural Biology Lab, School of Life Sciences, Jawaharlal Nehru University, New Delhi, India

Abstract

E. coli GroEL is a member of ATP-dependent chaperonin family and is involved in proper folding of cytosolic bacterial proteins. The *E. coli* GroEL contains 14 identical subunits of ~58.3 kD and arranged as two stalked rings. In current study, we have determined the X-ray structure of *E. coli* GroEL at 3.2-Å resolution. The GroEL protein was coexpressed during recombinant *M. tuberculosis* DprE1 protein expression in *E. coli* and was co-purified with DprE1. The GroEL-DprE1 complex was crystallized and x-ray structure analysis yielded electron density for only GroEL protein only and no density for DprE1 protein. Comparison of our GroEL structure with previous wild type GroEL (PDB-1XCK), DM-GroEL-(ATP)₁₄ (PDB-1KP₈) and GroEL- GroES-(ADP)₇ (PDB-1PF₉) structures have yielded the differences in (i) interactions between heptameric rings involved in allosteric signaling (ii) interactions within heptameric ring, (iii) H and I helices of apical domain involved in substrate binding and (iv) residues involved in signaling route. These results indicate that our GroEL structure may be in different state, which occurred during protein folding cycle after unloading the substrate and ADP.

Keywords: Molecular chaperone; GroEL; X-ray structure; Comparative structure analysis

Introduction

The GroEL protein is a member of ATP-dependent chaperonin family and promotes protein folding together with GroES protein [1]. The GroEL structure consists of 14 identical subunits of ~ 58.3 kD and arranged in two heptameric rings associated back-to-back on each other exhibiting D72 symmetry [2]. Each GroEL subunit contains three functional domains e.g., apical, intermediate and equatorial. The apical domain captures unfolded polypeptide and binds to GroES protein to encapsulate of substrate protein. The ATP-binding site is observed in equatorial domain of GroEL and equatorial domain forms contact between both heptameric rings. The intermediate domain of GroEL links apical domain to equatorial domain and flanked by hinge region. This hinge region allows the movement of polypeptide in response to ATP and GroES binding [2-4]. The GroEL and GroES proteins are essential for bacteriophage λ growth in *E. coli*. Cell [5]. The ATP binding to GroEL equatorial domain is required for GroES binding [6]. The coordinated ATP hydrolysis within heptameric ring of GroEL is required for release of protein substrate. The ATP binding to one GroEL subunit promotes ATP binding to another subunit within heptameric ring, but inhibits ATP binding to another heptameric ring. In earlier studies, several wild type GroEL crystal structures have been determined (PDB: 1XCK [7], 1SS8 [8], 1GRL [2], 2NWC [9], 1OEL [10]). Single particle cryoelectron microscopic analysis has yielded the *de novo* backbone tracing of native GroEL structure (PDB-3C9V) [11]. We have determined the crystal structure of wild type GroEL at 3.2 Å resolution in ADP and substrate unloaded state during crystallization experiment. We have compared our GroEL structure (PDB-4HEL) with previous wild type GroEL (PDB-1XCK) [7], DM-GroEL-(ATP)₁₄ (PDB-1KP₈) [12] and GroEL-GroES-(ADP)₇ (PDB-1PF₉) [13] crystal structures. Structural comparison analysis has shown significant differences in inter and intra heptameric rings contacts of GroEL protein, in H and I helices of apical domain involved in substrate binding and in residues involved in signaling route. These data suggest that our GroEL structure has occurred in different stage of protein folding cycle, when substrate and ADP is unloaded during crystallization experiment.

Materials and Methods

Protein purification and characterization

During recombinant dprE1 gene expression in *E. coli*, the GroEL protein co purified with DprE1 and eluted as DprE1-GroEL complex from Ni-NTA column. The *M. tuberculosis* dprE1 (Rv3790) gene was cloned in pET28a (+) vector and the resulting clone was used to transform *E. coli* BL21 (DE3) for protein expression. The cells were grown in luria-bertani media containing 25 µg/ml kanamycin at 37°C, until OD₆₀₀ reached to 0.5-0.6. The culture was induced with 0.1 mM IPTG at 25°C and grown further for 5 h at 25°C. The cells were harvested by centrifugation at 4000×g for 15 min at 4°C. The cell pellet was washed with 20 mM Tris-HCl pH 8.0, 150 mM NaCl, 0.1% triton-X100 and pelleted again by centrifugation. The pellet was resuspended in lysis buffer containing 20 mM Tris-HCl pH 8.0, 150 mM NaCl, 5% glycerol, 1 mM phenylmethylsulfonyl fluoride, 3 mM benzamidine-HCl, 3 mM β-mercapthanol, 10 mM imidazole, 0.2 mg/ml lysozyme and kept on ice for 1 h. The cells were lysed by sonication and centrifuged at 12,000×g for 30 min at 4°C. For purification, lysate was mixed with Ni-NTA resin and incubated for 2 Hours at cold room with rotating. Further resin was loaded in empty column and washed with buffer containing 25 mM Tris-HCl pH 8.0, 300 mM NaCl, 1 mM phenylmethylsulfonyl fluoride, 1 mM benzamidine-HCl, 1 mM 2-mercapthanol, 5% glycerol, and 35 mM imidazole. After washing, the protein was eluted in buffer containing 20 mM Tris-HCl pH 8.0, 150 mM NaCl, 0.25 mM phenylmethylsulfonyl fluoride, 2 mM benzamidine-HCl, 1 mM 2-mercapthanol, 5% glycerol and 300 mM

*Corresponding author: Ajay K Saxena, Room - 403/440, Structural Biology Lab, School of Life Sciences, Jawaharlal Nehru University, New Delhi-110 067, India, E-mail: ajaysaxena@mail.jnu.ac.in

Received June 10, 2016; Accepted June 20, 2016; Published June 27, 2016

Citation: Meena S, Saxena AK (2016) Crystal Structure of *Escherichia coli* GroEL in Substrate and ADP Unloaded State. J Phys Chem Biophys 6: 222. doi:10.4172/2161-0398.1000222

Copyright: © 2016 Meena S, et al. This is an open-access article distributed under the terms of the Creative Commons Attribution License, which permits unrestricted use, distribution, and reproduction in any medium, provided the original author and source are credited.

imidazole. The eluted protein fractions were pooled and concentrated using Amicon-10- Ultra centrifugal device (Millipore). The purified protein was analyzed on mass spectrometry, which indicated the presence of DprE1-GroEL protein. The complex protein was loaded on Sephacryl 200 (16/60) HR size exclusion column, pre-equilibrated with buffer containing 20 mM Tris-HCl pH 8.0, 150 mM NaCl, 4 mM 2-mercaptoethanol and 5% glycerol. The complex protein eluted in void volume of size exclusion column. The identity and purity of complex protein was checked on SDS-PAGE and mass spectrometry. The protein fractions were pooled and concentrated to 20 mg/ml by using Amicon- Ultra centrifugal device (Millipore).

Crystallization

Initial crystallization conditions were screened using Crystals Screen, Crystals Screen II and PEG/ION screen from Hampton Research. The crystallization experiments were performed using hanging and sitting drop vapor diffusion techniques at 4°C. In each trial, 0.2 µl of protein solution was mixed with 0.2 µl of precipitant solution and equilibrated against reservoir containing 100 µl of precipitant solution in 96 well plate. The microcrystals appeared in many crystallization conditions and these conditions were further optimized. Best crystals appeared in a drop containing 2 µl of protein solution mixed with 1 µl of precipitant solution containing 32% MPD, 100 mM Tris-HCl pH 7.5, 160 mM MgCl₂, 10% Glycerol and 2% (w/v) PEG6000. The crystals grew as rectangular bars with typical dimension of 0.6 × 0.4 × 0.3 mm (Figures 1A and 1B).

Intensity data collection and processing

For intensity data collection, single crystals were picked up from crystallization drop and flash-frozen in liquid nitrogen. The 32% MPD in precipitant solution worked as good cryo-protectant for diffraction measurements at cryogenic temperature. The native X-ray intensity data was collected using MAR225 CCD detector at BM14 beamline at ESRF, France. The reflections were indexed, integrated and scaled using *iMOSFLM* [14], *POINTLESS* and *SCALA* programs of CCP4 suite [15,16]. The *CTRUNCATE* program was used to generate *Fobs* and *FreeR* flag. The crystals belong to P2₁2₁2₁ space group and diffracted to 3.2 Å resolution. The details of intensity data collection and refinement statistics are given in Table 1.

Structure solution and refinement

The GroEL structure was determined by molecular replacement technique using wild type GroEL coordinate (PDB-1XCK) as initial model [7]. The Phaser [17] program of *Phenix* [18] suite was used for molecular replacement calculation. The structure was refined by *phenix.refine* [19] module and rebuilt using COOT [20] program. The *Fo-Fc* and *2Fo-Fc* electron density maps indicated no electron density for DprE1 protein and electron density of only GroEL protein was observed. The GroEL model was built by COOT program using composite omit map. All three mutated residues in wild type GroEL structure (PDB-1KP8) were refitted using COOT program. After refitting, the structure was refined by REFMAC [21] program of CCP4 suite [16] using all data between 50-3.2 Å resolutions. 5% of the data were kept for R_{free} calculation to monitor the progress of refinement. The final apo-GroEL structure was refined to R_{work} of 0.19 and R_{free} of 0.22. The quality of the model was checked by MolProbity [22] and PROCHECK [23]. Superpositions of GroEL structures were performed using LSQMAN program of CCP4 [16] suite. Figures were prepared by PyMOL [24].

Protein data bank accession codes

Coordinates and structure factor amplitudes have been deposited in PDB database with accession code (4HEL).

Results and Discussion

Overall structure of GroEL

During recombinant *M. tuberculosis* DprE1 protein expression, the GroEL protein was co-expressed together with DprE1 and purified using standard Ni-NTA and gel filtration chromatography (Figure 1A). The purified GroEL was analyzed on SDS-PAGE, which shows two proteins having small difference in molecular weight (Figure 1A). MALDI TOF-TOF mass spectrometric analysis on both bands shows the DprE1 and GroEL proteins. The crystal structure of GroEL trapped with its substrate during protein folding process is still lacking. We performed the crystallization experiments on DprE1-GroEL complex and obtained the rectangular shaped crystals of GroEL (Figure 1B). Native X-ray intensity dataset was collected at 3.2 Å resolution and structure analysis has yielded only GroEL structure with no electron density for DprE1 protein. The GroEL crystals belong to P2₁2₁2₁ space group with one GroEL molecule in asymmetric unit. The GroEL

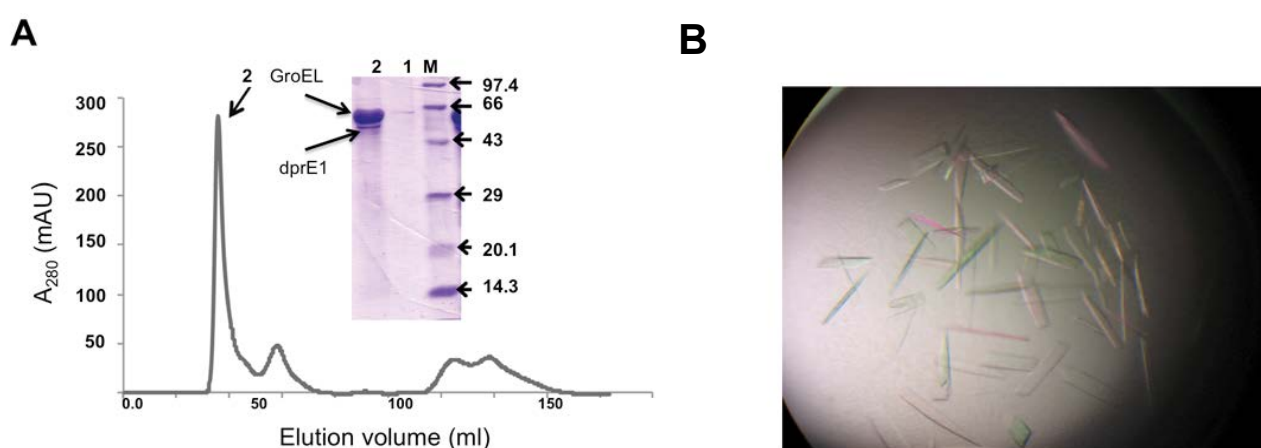


Figure 1: (A) Gel filtration chromatogram and SDS-PAGE analysis of purified GroEL-DprE1 complex. (B) Rectangular shaped crystals of GroEL.

Beamline	BM ₁₄ , (ESRF)
Wavelength (Å)	0.97327
Temperature	100 K
Space group	P2 ₁ 2 ₁ 2 ₁
Unit cell parameters (Å, 0)	a=136.2, b=261.8, c=282.3
Resolution range Å	59.38-3.20 (3.37-3.20)
Total observations	12,47,571
Unique observations	166,588 (24,106)
Multiplicity	7.5 (7.3)
Completeness	100 (100)
I/σ (I)	6.1 (2.4)
R _{merge}	0.32 (0.85)
Molecules/AU	1
Solvent content, Matthew's coefficient	62%, 3.27 Å ³ /Da
Refinement statistics	
R _{factor} (work/free)	0.19/0.22
Protein atoms	53,970
Mean B factor(Å ²)	48.2
r.m.s deviation bond (Å)	0.015
r.m.s deviation angle (0)	1.647
Ramachandran plot	
Most Favored regions (%)	91.1
Additional allowed regions (%)	7.4
Generously allowed regions (%)	0.8
Disallowed region (%)	0.8

Values in parentheses describe the highest resolution shell.

$R_{merge} = \frac{\sum_h \sum_i |I_{h,i} - \langle I_h \rangle|}{\sum_h \sum_i I_{h,i}}$, where $I_{h,i}$ is the i^{th} intensity measurement of reflection h and

$\langle I_h \rangle$ is the average intensity of that reflection. $R_{factor} = \frac{\sum_h k |F_{obs}(hkl) - F_{calc}(hkl)|}{\sum_h k F_{obs}(hkl)}$

Table 1: Intensity data collection and refinement statistics.

structure was determined by molecular replacement technique using wild type GroEL structure (PDB-1XCK) [7] as input. The GroEL structure was refined to Rfactor of 0.19 and Rfree of 0.22 and contains 7364 residues (14 × 526 residues in each subunit). Both heptameric rings of GroEL are stalked back-to-back using equatorial domain as interface. Mg²⁺ and K⁺ ions are required for ATP binding, hydrolysis and cooperatively between inter and intra heptameric rings of GroEL [12,25,26]. The ion-binding sites in GroEL were identified using thallium ions (Tl⁺) replacement [27]. Electron densities of these ions are not observed in our GroEL structure, though MgCl₂ was used in crystallization buffer.

Structural changes in apical domain

We have superposed the backbone Ca atoms of all 14 subunits of our GroEL structure using equatorial domain as reference (Figure 2A). It yielded maximum r.m.s.d. of 7.2 Å for apical domain and rest of structure superposed well. When Ca atoms of all 14 subunits of GroEL were superposed to each other, following conformational changes e.g., 12.3° for apo-GroEL (PDB-1XCK) [7], 7.4° for DM-GroEL-(ATP)₁₄ (PDB-1KP8) [12] and 2.1° for GroEL-GroES-(ADP)₇ (PDB-1PF9) [13] structures were observed in apical domain. The GroEL is composed of two heptameric rings and each ring consists of 7 fold symmetry [2]. Deviation from ideality in GroEL structure shows variability in perfect symmetry with its all domain [8]. Equatorial domain of GroEL is most stable and highly symmetric in nature due to less mobility and little conformational change. The GroEL apical domain is highly mobile in nature, as it interacts with native polypeptide. The GroEL apical domain goes into a series of conformational changes with a little conformational change in intermediate domain [28,29].

Contacts within heptameric ring

Several structural changes are occurred in GroEL during protein folding cycle, in which many bonds are broken and new bonds are formed [17]. These bonds are formed within heptameric ring and between both heptameric rings of GroEL. In a recent study [17], the switch between trajectory of protein folding cycle is dissected [17]. As shown in Figure 2B, specific inter-domain interactions are observed, which stabilize the monomeric GroEL structure. Arg58(Nη2) of equatorial domain forms hydrogen bond with Pro208(O') of apical domain (~2.4 Å). Asp83(Oδ2) of apical domain forms hydrogen bond with Ser79(N) of equatorial domain (2.7 Å). In all 14 subunits, Lys327(Nζ) of apical domain forms salt bridge with Ser79(OH) and also with Asp83(Oδ2) in few cases. The interactions between heptameric rings play key role in release of substrate and ADP during protein folding cycle. Interactions between apical to equatorial domains provide compactness to overall GroEL structure, when it needs to rearrange itself in proper conformation for trapping unfolded polypeptide in next cycle.

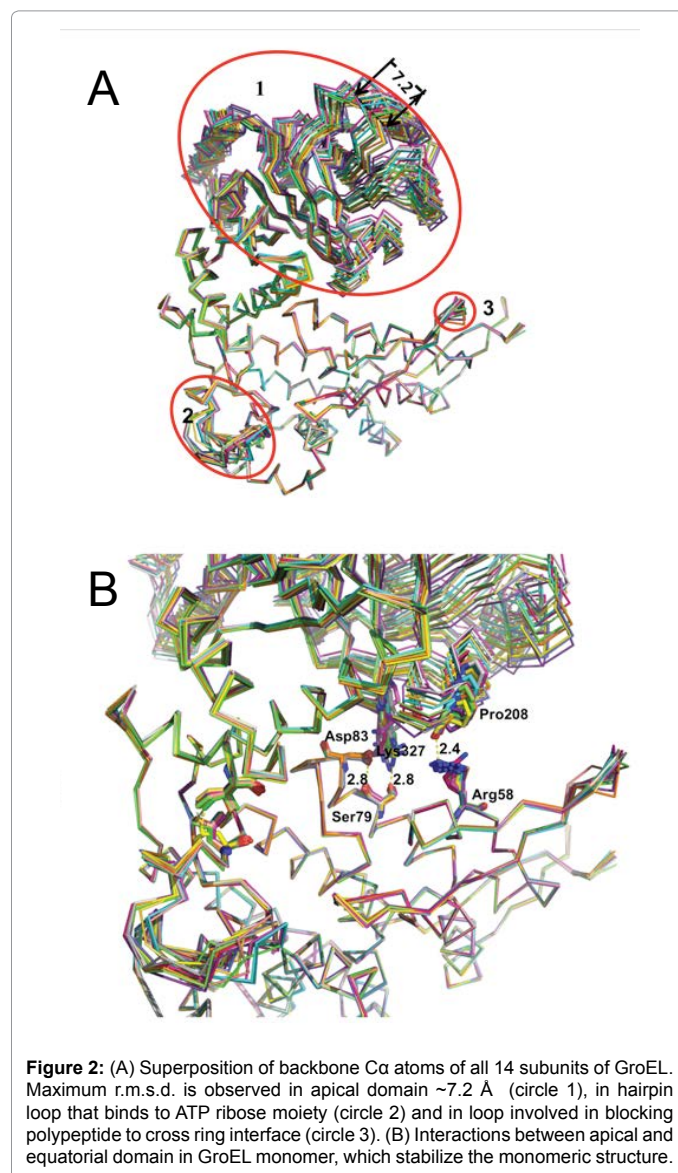


Figure 2: (A) Superposition of backbone Ca atoms of all 14 subunits of GroEL. Maximum r.m.s.d. is observed in apical domain ~7.2 Å (circle 1), in hairpin loop that binds to ATP ribose moiety (circle 2) and in loop involved in blocking polypeptide to cross ring interface (circle 3). (B) Interactions between apical and equatorial domain in GroEL monomer, which stabilize the monomeric structure.

Interactions between two GroEL subunits within heptameric ring are shown in Figure 3B. The contact distances between heptameric rings in our GroEL structure are different than apo- GroEL structure obtained by cryo-electron microscopy [17]. In TT state, when GroEL is not bound to ATP and naïve polypeptide, the average distance between Arg197(N η 1) to Glu386(O ϵ 1) was 4.6 Å in CryoEM structure [17]. Current distance is 3.2 Å in our GroEL structure, which indicates more closer subunit interaction. Contact distance of another switch bond Glu255(O ϵ 1) to Lys207(N ζ) was 4.0 Å in apo-GroEL structure by Clare et al. [17]. Same contact distance is 7.5 Å in our GroEL structure. It indicates that our GroEL structure is not in native stage, but in a different stage of protein folding cycle. The hydrophobic collar of GroEL is involved in trapping non-native polypeptide to fold them properly [12,29,30]. Three domains of GroEL monomer interact specifically with three domains of adjacent GroEL monomer. In Figure 3B, Glu386(O ϵ 1) of apical domain of one monomer forms salt bridge with Arg197(N η 1) of intermediate domain of next monomer (3.2 Å), which has been proposed in positive allostery [30]. Lys226(N ζ) of apical domain forms salt bridge with Glu216(O δ 1) of adjacent apical domain (3.0 Å). Asp283(N) of apical domain forms hydrogen bond with Thr181(O *) of adjacent apical domain (3.1 Å). These interactions

are broken during ATP and polypeptide binding to GroEL. During recycling, these contacts further stabilize the GroEL structure needed for next cycle. Interactions between equatorial domain of two GroEL monomers are shown in Figure 3C. Leu513(O *) forms hydrogen bond with Asn37(N δ 2) of adjacent subunit. Lys4(N ζ 2) forms hydrogen bond with Glu59(O *) (3.0 Å) and Lys4(N) forms hydrogen bond with Glu61(O *) (2.7 Å). Glu61(O ϵ 2) forms hydrogen bond with Ala2(N) (3.1 Å). These interactions are observed in loops extended at ring interface and between subunit-subunit contacts. Distances of all other interactions are given in Figure 3C. Contacts between two adjacent equatorial domains of same ring are needed for signaling between GroEL subunits. These interactions stabilize the ring-ring interface during expansion at the time of cycling [17,31]. These interactions are also observed in apo-GroEL (PDB-1XCK) [7] and DM-GroEL-(ATP)₁₄ (PDB-1KP8) [12] structures having different bond lengths than our GroEL structure (PDB-4HEL).

Contacts between both heptameric rings

Contacts between heptameric rings are important for inter-ring signaling of GroEL and have been studied extensively [2,7,28,32,33]. We have observed different inter-ring contacts than previous GroEL structures. One GroEL subunit of top ring interacts with two subunits of bottom ring in 1:2 stoichiometry, termed as left and right of top ring [2]. On right site of Figure 4, Arg452(N η 2) of top ring forms salt bridge with Glu461(O ϵ 1) of bottom ring (3.5 Å), and Glu461(O δ 1) of top ring forms salt bridge with Arg452(N η 2) of bottom ring (3.9 Å). These interactions play key role in signaling and temperature sensing [17,34,35]. The distances of these contacts are similar in GroEL structure in TT state [7,24], but little different in our GroEL structure (PDB-4HEL) and in apo-GroEL (PDB-1XCK) and DM-GroEL-(ATP)₁₄ (PDB-1KP8) structures [7,12] (Figure 4). On left site of Figure 4, Asn112 is located at the loop connected with helix, where Ala109 is located and play key role in the left site of contact [2,17]. Ala109 of top ring contacts Ala109 of bottom ring with average distance of 4.0 Å.

Superposition of our GroEL structure (PDB-4HEL) with apo-GroEL (PDB-1XCK), DM- GroEL-(ATP)₁₄ (PDB-1KP8) and GroEL-GroES-(ADP)₇ (PDB-1PF9) structures

Superposition of backbone Ca atoms of our GroEL structure (PDB-4HEL) with previous wild type GroEL structure (PDB-1XCK)₇, has yielded the r.m.s.d. of 0.89 Å. Most of the structure is superposed, but significant deviations are observed in H and I helices involved in naïve polypeptide binding [12,36,37]. Superposition of backbone Ca atoms of our GroEL structure with DM-GroEL-(ATP)₁₄ structure gave r.m.s.d. of 1.59 Å. DM-GroEL-(ATP)₁₄ structure looks elevated at apical domain, little at intermediate domain than our GroEL structure, consistent with earlier observation [36,38]. Superposition with our GroEL structure with GroEL-GroES-(ADP)₇ structure gave r.m.s.d. of 1.01 Å, more than wild type GroEL structure (PDB-1XCK). To know whether both heptameric rings of our GroEL structure are in symmetry with TT state, we superposed both heptameric rings of our GroEL structure and observed the r.m.s.d. of 0.55 Å, similar to previous apo-GroEL structure (PDB-1XCK). It indicates that both rings of our GroEL structure are not in perfect TT state and having some deviation from ideality in H and I helices of apical domain.

Factor analysis

Our GroEL structure has overall B factor of 49.9 Å² and maximum deviation is observed in apical domain. We superposed 14 subunits of our GroEL structure using equatorial domain as reference and

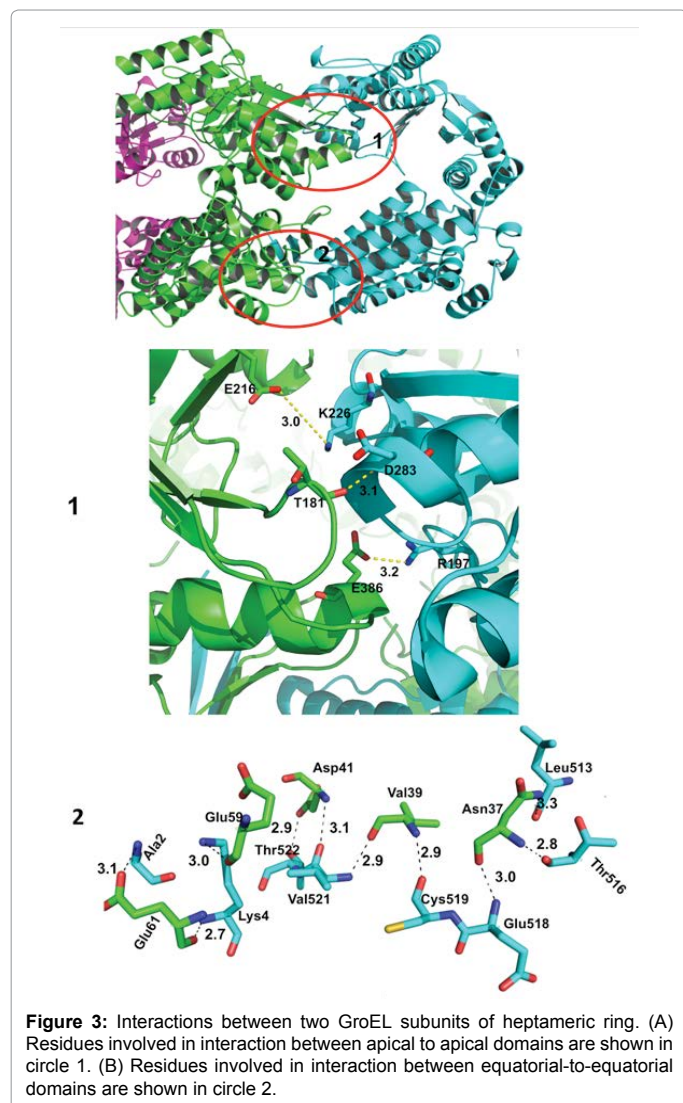


Figure 3: Interactions between two GroEL subunits of heptameric ring. (A) Residues involved in interaction between apical to apical domains are shown in circle 1. (B) Residues involved in interaction between equatorial-to-equatorial domains are shown in circle 2.

observed high B factor for apical domain (Figure 5). Apart from apical domain, two- hairpin loop of equatorial domain also contain high B factor. As shown circle 1 of Figure 5, hairpin loop interacts with ATP's ribose moiety. In DM-GroEL-(ATP)₁₄ (PDB-1KP8) [12] structure, this loop is well ordered, but contains high B factor in our GroEL structure. It indicates the role of ATP in stabilizing this loop, which may work as lid for ATP to enter and release. Another loop at central channel of interface of two rings has high B factor. It may work as barrier for peptide crossing at interface of two rings. GroEL asymmetry is measured and refined by TLS refinement by Chaudhary et al. [8] and found maximum at apical domain. It shows greater flexibility, highly mobile for binding naïve polypeptide and shows high domain movement during folding cycle.

Residues involved in signaling route

In Figure 6, Arg13(Nη1) forms hydrogen bonds with Glu518(Oε2) of same GroEL subunit (2.6 Å). In earlier apo-GroEL structure [7], Arg13(Nη1) also forms hydrogen bonds with Glu518(Oε2) of same subunit (2.8 Å). Arg36(Nη1) forms salt bridges with Glu518(Oε1) (2.9 Å) and Asn457(Oδ1) (3.0 Å). Contact distances between Arg36(Nη1) to Glu518(Oε1) of adjacent subunit was 2.8 Å in GroEL-GroES-(ADP)₇ structure (PDB-1PF9), 4.4 Å in apo-GroEL structure (PDB-1XCK) and 4.2 Å in DM-GroEL-(ATP)₁₄ structure (PDB-1KP8). The Asn457(Nδ1) forms hydrogen bond with Leu31(O') and Leu31 is the neighbor of Gly32 that contact directly with ATP. Asn457 and Arg36 contacts at interface of two subunit of same ring. It may play a role in positive co-operativity in ring and pass information to helix P, where Arg452 is located. Arg452 is the key residue for interface signaling. On the right site, Arg452(Nη1) forms salt bridge Glu461(Oε1) (3.9 Å) and Glu461(Oε1) form salt bridge with Arg452(Nη1) (3.8 Å) of opposite ring. The contact distance of Arg452(Nη1)-- Glu461(Oε1) was 3.4 Å in apo-GroEL structure (PDB-1XCK), 3.4 Å in DM- GroEL-(ATP)₁₄ structure (PDB-1KP8) and 4.9 Å in GroEL-GroES-(ADP)₇ structure (PDB-1PF9). The contact distance of Glu461(Oε1) ---- Arg452(Nη1) was 4.6 Å in apo-GroEL structure (PDB-1XCK), 4.6 Å in DM-GroEL-

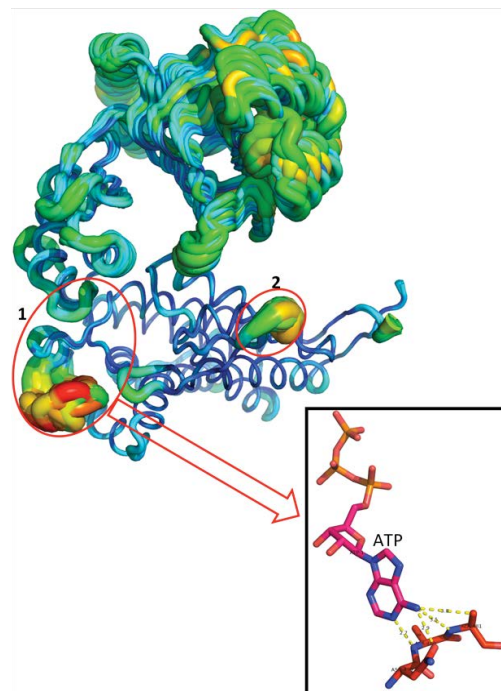


Figure 5: B factor analysis of all 14 subunits of our apo-GroEL structure. Maximum B factor is observed in apical domain, which is highly mobile and involved in polypeptide binding. In two other loops of equatorial domain, involved in ATP binding and interface barrier. Inset shows ATP interactions with loop.

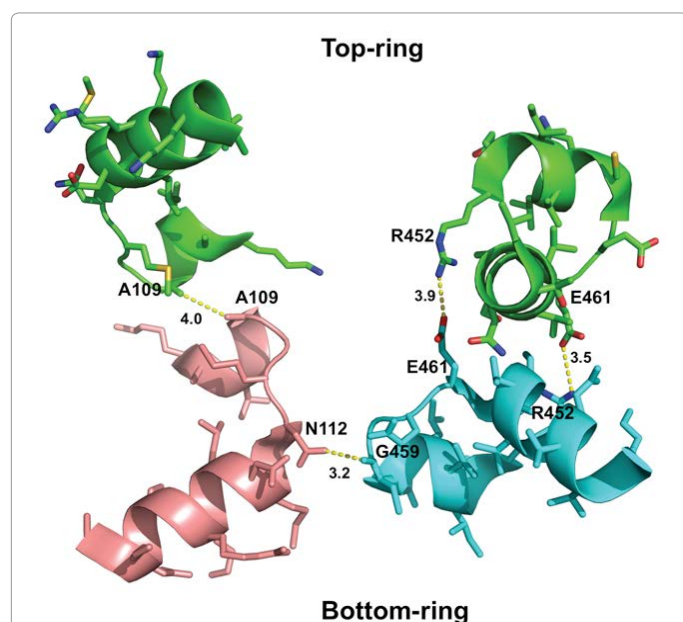


Figure 4: Interactions between GroEL heptameric rings, defined as left and right hand of top ring. (A) Inter ring residues involved in interactions on left hand (B) Inter ring residues involved in interactions on right hand.

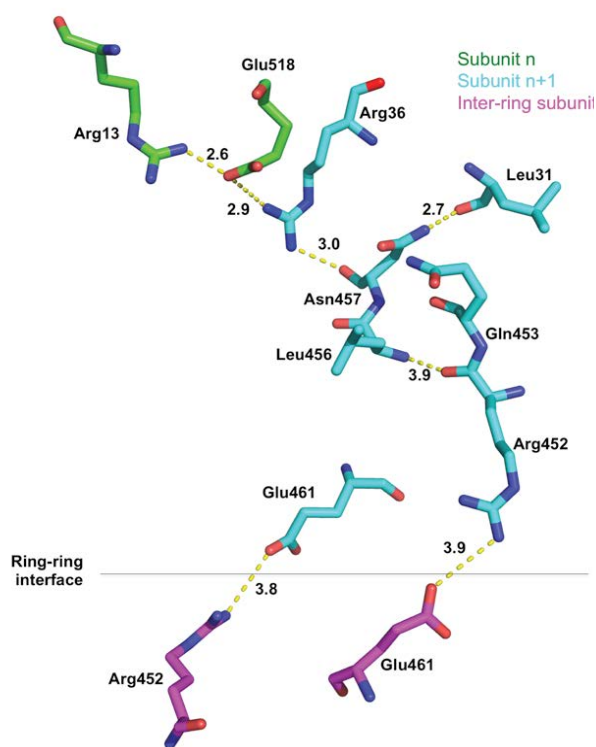


Figure 6: Interactions between residues involved signaling route of GroEL. Interactions between residues involved in intra and inter ring signaling of GroEL. Salt bridges are shown in broken lines.

(ATP)₁₄ structure (PDB-1KP8) and 2.8 Å in GroEL-GroES-(ADP)₇ structure (PDB-1PF9).

Conclusion

In summary, we have determined the crystal structure wild type *E. coli* GroEL at 3.2 Å resolution in substrate and ADP unloaded state. Comparison of our GroEL structure with previous wild type GroEL (PDB-1XCK), DM-GroEL-(ATP)₁₄ (PDB-1KP8) and GroEL-GroES-(ADP)₇ (PDB-1PF9) structures have yielded significant differences in (i) interactions between heptameric rings involved in allosteric signaling (ii) interactions within heptameric ring (iii) H and I helices of apical domain involved in substrate binding and (iv) interactions between residues involved signaling route of GroEL. These results indicate that our GroEL structure exists in different stage of protein folding cycle, when substrate and ADP is unloaded. In crystal structure some time difference in the contact distance and little change also observed due to the crystal packing contacts but in our case we also compared with apo-GroEL [7] that has same space group (P2₁2₁2₁) and having same space group and this much of difference is highly unlike possibility.

Acknowledgements

SitaRam Meena was supported by senior research fellowship of Department of Biotechnology, Government of India, New Delhi, India. Ajay K Saxena is supported by funds from UGC networking, Capacity buildup and DST - purse grant from Jawaharlal Nehru University, New Delhi, India. The funding for current work was supported by Department of Biotechnology, India.

References

- Houry WA, Frishman D, Eckerskorn C, Lottspeich F, Hartl FU (1999) Identification of in vivo substrates of the chaperonin GroEL. *Nature* 402: 147-154.
- Braig K, Otwinowski Z, Hegde R, Boisvert DC, Joachimiak A, et al. (1994) The crystal structure of the bacterial chaperonin GroEL at 2.8 Å. *Nature* 371: 578-586.
- Fenton WA, Horwich AL (1997) GroEL-mediated protein folding. *Protein Sci* 6: 743-760.
- Boisvert DC, Wang J, Otwinowski Z, Horwich AL, Sigler PB (1996) The 2.4 Å crystal structure of the bacterial chaperonin GroEL complexed with ATP gamma S. *Nat Struct Biol* 3: 170-177.
- Horwich AL, Farr GW, Fenton WA (2006) GroEL-GroES-mediated protein folding. *Chem Rev* 106: 1917-1930.
- Chandrasekhar GN, Tilly K, Woolford C, Hendrix R, Georgopoulos C (1986) Purification and properties of the groES morphogenetic protein of *Escherichia coli*. *J Biol Chem* 261: 12414-12419.
- Bartolucci C, Lamba D, Grazulis S, Manakova E, Heumann H (2005) Crystal structure of wild-type chaperonin GroEL. *J Mol Biol* 354: 940-951.
- Chaudhry C (2004) Exploring the structural dynamics of the *E. coli* chaperonin GroEL using translation-libration-screw crystallographic refinement of intermediate states. *J Mol Biol* 342: 229-245.
- Kiser PD, Lodowski DT, Palczewski K (2007) Purification, crystallization and structure determination of native GroEL from *Escherichia coli* lacking bound potassium ions. *Acta Crystallogr Sect F Struct Biol Cryst Commun* 63: 457-461.
- Braig K, Adams PD, Brünger AT (1995) Conformational variability in the refined structure of the chaperonin GroEL at 2.8 Å resolution. *Nat Struct Biol* 2: 1083-1094.
- Ludtke SJ, Baker ML, Chen DH, Song JL, Chuang DT, et al. (2008) De novo backbone trace of GroEL from single particle electron cryomicroscopy. *Structure* 16: 441-448.
- Wang J, Boisvert DC (2003) Structural basis for GroEL-assisted protein folding from the crystal structure of (GroEL-KMgATP)₁₄ at 2.0 Å resolution. *J Mol Biol* 327: 843-855.
- Xu Z, Horwich AL, Sigler PB (1997) The crystal structure of the asymmetric GroEL-GroES-(ADP)₇ chaperonin complex. *Nature* 388: 741-750.
- Battye TG, Kontogiannis L, Johnson O, Powell HR, Leslie AG (2011) iMOSFLM: a new graphical interface for diffraction-image processing with Mosflm. *Acta Crystallogr D Biol Crystallogr* 67: 271-281.
- Evans PR (2011) An introduction to data reduction: space-group determination, scaling and intensity statistics. *Acta Crystallogr D Biol Crystallogr* 67: 282-292.
- Winn MD, Ballard CC, Cowtan KD, Dodson EJ, Emsley P, et al. (2011) Overview of the CCP4 suite and current developments. *Acta Crystallogr D Biol Crystallogr* 67: 235-242.
- McCoy AJ, Grosse-Kunstleve RW, Adams PD, Winn MD, Storoni LC, et al. (2007) Phaser crystallographic software. *J Appl Crystallogr* 40: 658-674.
- Adams PD, Afonine PV, Bunkóczi G, Chen VB, Davis IW, et al. (2010) PHENIX: a comprehensive Python-based system for macromolecular structure solution. *Acta Crystallogr D Biol Crystallogr* 66: 213-221.
- Afonine PV, Grosse-Kunstleve RW, Echols N, Headd JJ, Moriarty NW, et al. (2012) Towards automated crystallographic structure refinement with phenix refine. *Acta Crystallogr D Biol Crystallogr* 68: 352-367.
- Emsley P, Lohkamp B, Scott WG, Cowtan K (2010) Features and development of Coot. *Acta Crystallogr D Biol Crystallogr* 66: 486-501.
- Murshudov GN, Skubák P, Lebedev AA, Pannu NS, Steiner RA, et al. (2011) REFMAC5 for the refinement of macromolecular crystal structures. *Acta Crystallogr D Biol Crystallogr* 67: 355-367.
- Chen VB, Arendall WB 3rd, Headd JJ, Keedy DA, Immormino RM, et al. (2010) MolProbity: all-atom structure validation for macromolecular crystallography. *Acta Crystallogr D Biol Crystallogr* 66: 12-21.
- Laskowski RA (1993) PROCHECK: a program to check the stereochemical quality of protein structures. *J Appl Cryst* 26: 283-291.
- Schrodinger LLC (2010) The PyMOL Molecular Graphics System. Version 1.3r1. 2010.
- Grason JP (2008) Setting the chaperonin timer: the effects of K⁺ and substrate protein on ATP hydrolysis. *Proc Natl Acad Sci USA* 105: 17334-17338.
- Viitanen PV (1990) Chaperonin-facilitated refolding of ribulosebisphosphate carboxylase and ATP hydrolysis by chaperonin 60 (groEL) are K⁺ dependent. *Biochemistry* 29: 5665-5671.
- Kiser PD, Lorimer GH, Palczewski K (2009) Use of thallium to identify monovalent cation binding sites in GroEL. *Acta Crystallogr Sect F Struct Biol Cryst Commun* 65: 967-971.
- Clare DK, Vasishtan D, Stagg S, Quispe J, Farr GW, et al. (2012) ATP-triggered conformational changes delineate substrate-binding and -folding mechanics of the GroEL chaperonin. *Cell* 149: 113-123.
- Weissman JS, Hohl CM, Kovalenko O, Kashi Y, Chen S, et al. (1995) Mechanism of GroEL action: productive release of polypeptide from a sequestered position under GroES. *Cell* 83: 577-587.
- White HE, Chen S, Roseman AM, Yifrach O, Horovitz A, et al. (1997) Structural basis of allosteric changes in the GroEL mutant Arg197->Ala. *Nat Struct Biol* 4: 690-694.
- Clare DK, Bakkes PJ, van Heerikhuizen H, van der Vies SM, Saibil HR (2009) Chaperonin complex with a newly folded protein encapsulated in the folding chamber. *Nature* 457: 107-110.
- Roseman AM, Chen S, White H, Braig K, Saibil HR (1996) The chaperonin ATPase cycle: mechanism of allosteric switching and movements of substrate-binding domains in GroEL. *Cell* 87: 241-251.
- Clare DK, Stagg S, Quispe J, Farr GW, Horwich AL, et al. (2008) Multiple states of a nucleotide-bound group 2 chaperonin. *Structure* 16: 528-534.
- Cabo-Bilbao A, Spinelli S, Sot B, Agirre J, Mechaly AE, et al. (2006) Crystal structure of the temperature-sensitive and allosteric-defective chaperonin GroEL461K. *J Struct Biol* 155: 482-492.
- Ranson NA, Clare DK, Farr GW, Houldershaw D, Horwich AL, et al. (2006) Allosteric signaling of ATP hydrolysis in GroEL-GroES complexes. *Nat Struct Mol Biol* 13: 147-152.
- Rye HS, Roseman AM, Chen S, Furtak K, Fenton WA, et al. (1999) GroEL-GroES cycling: ATP and nonnative polypeptide direct alternation of folding-active rings. *Cell* 97: 325-338.
- Chen Y, Ding F, Nie H, Serohijos AW, Sharma S, et al. (2008) Protein folding: then and now. *Arch Biochem Biophys* 469: 4-19.
- Ma J, Sigler PB, Xu Z, Karplus M (2000) A dynamic model for the allosteric mechanism of GroEL. *J Mol Biol* 302: 303-313.